

PAPER • OPEN ACCESS

Atomistic molecular dynamics simulation of grapheneisoprene nanocomposites

To cite this article: P Chanlert *et al* 2018 *J. Phys.: Conf. Ser.* **1144** 012074

View the [article online](#) for updates and enhancements.



IOP | ebooks™

Bringing you innovative digital publishing with leading voices to create your essential collection of books in STEM research.

Start exploring the collection - download the first chapter of every title for free.

Atomistic molecular dynamics simulation of graphene-isoprene nanocomposites

P Chanlert¹, J Wong-Ekkabut², W Liewrian^{3,4,5} and T Sutthibutpong^{3,4,5*}

¹ Program of Physics, Faculty of Science and Technology, Songkhla Rajabhat University, Songkhla, 90000, Thailand

² Department of Physics, Faculty of Science, Kasetsart University, Bangkok 10900, Thailand

³ Theoretical and Computational Physics Group, Department of Physics, Faculty of Science, King Mongkut's University of Technology Thonburi (KMUTT), Bangkok 10140, Thailand

⁴ Theoretical and Computational Science Center (TaCS), Science Laboratory Building, Faculty of Science, King Mongkut's University of Technology Thonburi (KMUTT), Bangkok 10140, Thailand

⁵ Thailand Center of Excellence in Physics (ThEP Center), Commission on Higher Education, Bangkok 10400, Thailand

*email: thana.sut@mail.kmutt.ac.th

Abstract. A series of atomistic molecular dynamics simulations were performed for 4-mer isoprene molecules confined between graphene sheets with varied graphene separations in order to observe the finite size effects arose from the van der Waals interactions between the isoprene oligomer, forming high density shells at the graphene interfaces. For the small confinement regions, 1.24 nm and 2.21 nm, local density of isoprene at the graphene interface becomes higher than 10 times the bulk density. These results provided the further insights towards the rational design of nanostructures based on graphene sheets and natural rubber polymer.

1. Introduction

Composite material is the combination between two materials or more where chemical reaction between these materials is absent. In composites, one with higher quantity is called matrix while those with lesser quantity are called fillers. In general, adding fillers into matrix material enhances both physical and mechanical properties in some ways. However, the quantity of filler added to composites plays an important role in determining properties. To get the required physical and mechanical properties, determining an optimal ratio between fillers and matrix is necessary.

Composites where, at least, one of components shows dimensions in the nanometer scale, is called 'Nanocomposites'. Since properties of a material in nanoscale is almost totally different from the itself in macro- or microscopic scale.

Polymer is a macromolecular compound with repeating unit. It is one of material types well-known for being used in various industries due to its versatile properties depending on based monomer, molecular arrangement, degree of crystallinity, and so on. Different polymerization process and cooling profile of molten polymer can result in different organization. Degree of crystallinity is resulted from these factors. Higher degree of crystallinity improves properties such as strength, stability, chemical



resistance etc. However, the more crystalline a material is, the less light can pass through it resulting in more translucent and opaque.

Graphene-polymer nanocomposites have attracted some attentions recently due to its ability to be used in potential applications as a stress sensor or a lightweight-flexible conductor and the mechanical reinforcement due to the filler addition [1, 2, 3].

Atomistic molecular dynamic simulations served as a powerful tool for the studies of nanocomposite material structures due to their reasonable ability to reproduce the macroscopic properties measured from the experiments. The verified atomistic details were then provided to gain insights on the molecular mechanisms underlying macroscopic changes [4, 5].

In this work, we set up simple nanocomposite systems with a rather short oligomer chain, as the microscopic phenomena could still be observed with a relatively low computational cost. Three atomistic molecular dynamics (MD) simulations of three different numbers of isoprene 4-mer (isoprene tetramer) molecules confined within an infinitely large graphene sheet under room temperature and atmospheric pressure. Local density and chain orientation were analyzed to elucidate the microscopic behaviors of the isoprene 4-mer chains at the graphene/isoprene interface and between two separated graphene.

2. Methodology

2.1 Starting Structures and topologies

The starting structure of a 4-mer cis-isoprene was built by the program Avogadro [6] Then, a 4nm x 4nm graphene sheet was built by a Nanotube Builder module implemented in the Visual Molecular Dynamics (VMD) program. The sheet contained 678 carbon atoms. After that, the topology files of both 4-mer isoprene and graphene were generated from the Automated Topology Builder (ATB) webserver [7]. The GROMOS54A7 forcefield parameters containing information on the covalent bonds and van der Waals radii were used.

2.2 MD Simulation Setup

With the starting structures and topology files prepared in section 2.1, rectangular simulation boxes were built so that the dimension in the xy-plane could accommodate the virtually infinite graphene sheet when periodic boundary conditions were applied. Then, 30, 60 and 120 isoprene 4-mer molecules were added for each of the three simulations, corresponding to 100, 50 and 25 per hundred rubbers (phr) of graphene concentration. The simulation box of the system of graphene with 30 4-mer was doubled by duplicating the numbers of both graphene and isoprene 4-mer. Energy minimization by steepest-descent method was done for each structure before the first-step 50-picosecond equilibration under constant number of atoms, volume and temperature (*NVT*) at 300 K. The temperature was regulated by the velocity rescale algorithm. The LINCS holonomic constraints [8] were applied so that the timestep of 2 femtosecond (fs) was allowed. The particle mesh Ewald (PME) method [9] were used to treat the long-range interactions and a cutoff distance of 10 Å were used for van der Waals interactions. After that, during the second step 200-picosecond equilibration, Parrinello-Rahman semi-isotropic pressure coupling [10] was switched on for the equilibration at constant number of atoms, pressure and temperature (*NPT*) at 1 atm and 300 K. The system compressibility for xy-plane was set to 0 so that the xy-plane dimensions were kept constant. The structures obtained from NPT equilibrations were shown in Figure 1 and the information on all the simulations performed was given in Table 1. Finally, a 50-nanosecond long productive MD run was performed for each structure to generate many sample snapshots for the conformational analysis. All calculations were performed by GROMACS 5.1.2 [11].

2.3 Analysis

Local isoprene density along the z-axis defined in Figure 1 and Figure 2 was obtained from counting the number of carbon atoms found in each slab of thickness $\Delta\phi = 0.02$ nm. The total carbon mass in each slab was rescaled by the factor 68/60 in order to take into account the hydrogen atoms and was then divided by the volume. The calculated density in each slab was plotted as a function of z.

Chain orientation of a 4-mer isoprene molecule in this work was quantified by an angle made by the graphene plane and the vector between a representative carbon atom (C2) from the second monomer and another representative carbon atom (C3) from the third monomer. Probability distribution of the defined orientation angle was plotted for each simulation.

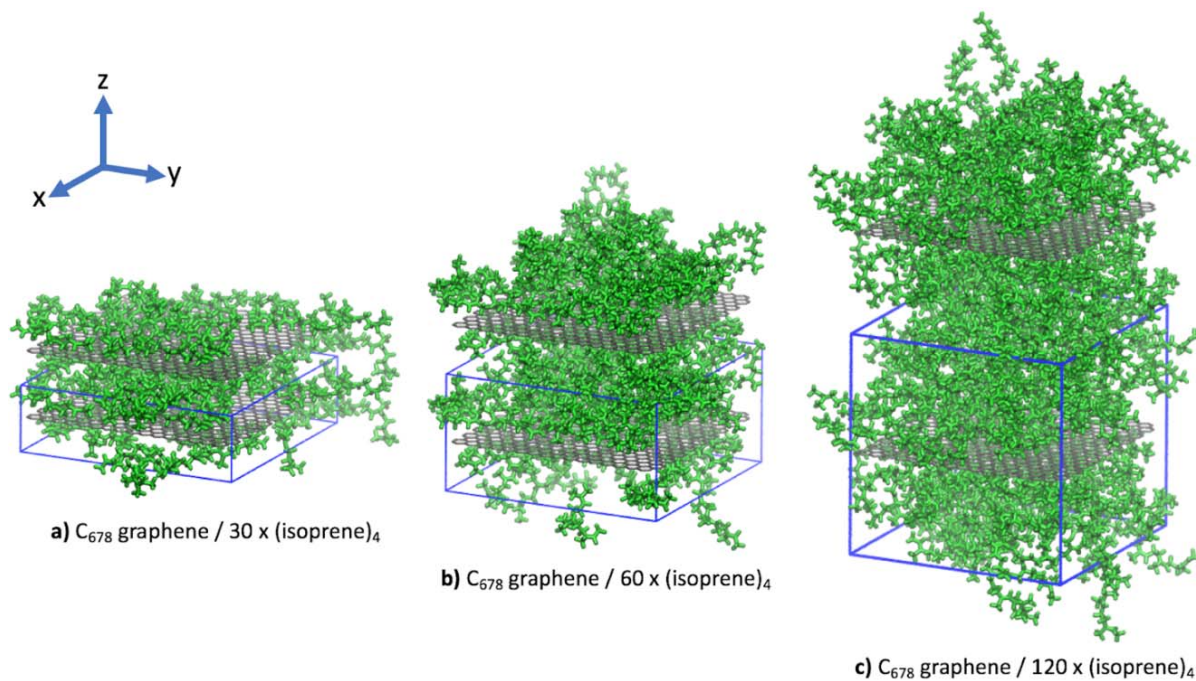


Figure 1. structures of graphene / 4-mer isoprene composites after an *NPT* equilibration a) C₆₇₈ graphene / 30 x (isoprene)₄, b) C₆₇₈ graphene / 60 x (isoprene)₄ and c) C₆₇₈ graphene / 120 x (isoprene)₄

3. Results and Discussions

Atomistic molecular dynamics simulations were performed on the systems containing different per hundred rubber (phr) ratios between parallel graphene sheets and isoprene 4-mer with varied graphene separation distances.

According to Table 1, total density of the composites increased with higher graphene concentration. The density was found to drop from $1228 \text{ kg} \cdot \text{m}^{-3}$ for the system with 1.24 nm graphene separation distance to $928 \text{ kg} \cdot \text{m}^{-3}$ for 4.11 nm, as the larger the graphene separation was, the less dominantly graphene mass affected the system density. It could be implied that, at a very large graphene separation, total density of the composites would approach the density of the bulk isoprene at around $800 \text{ kg} \cdot \text{m}^{-3}$. However, the contribution of isoprene to system density was found to decrease with smaller graphene separation distance. This was due to the uniform spacings of about 0.4 nm observed between center of mass of graphene atoms and isoprene atoms at the interface, signifying the averaged van der Waals radius of carbon atoms in graphene and in isoprene. These spacing become dominant when graphene separation distance is small, resulting in the decrease of density contribution from isoprene.

According to Figure 2, local density profile of isoprene for each graphene separation distance was plotted as a function of cross-section distance along the *z*-axis. The position where the graphene plane was located displayed zero density. At the edge of the isoprene inaccessible areas on both sides of graphene planes, isoprene density became maximum for all separation distances. For the system with 4.11 nm graphene separation, the high-density shells at the interface with peak density around 3 times the bulk isoprene density were found. Peak density of the next high-density shells was lower at further distance from graphene and were converging towards bulk density.

At smaller graphene separation (2.21 nm and 1.24 nm). The first peak densities were found over 10 times the bulk density. The big difference between the density local minima and local maxima suggested that the isoprene morphology became more crystal-like with smaller separation distance.

The highly-ordered conformation at the high-density shells was demonstrated in Figure 3, when orientations of the chain vectors relative to the graphene plane were determined. Chain vectors were defined by pairs of terminal carbon atoms of second and third monomers (see Figure 3a). In Figure 3b, the probability distributions of orientation angles (ϕ) between chain vectors and a graphene plane for each graphene separation distance was plotted. This plot demonstrated the influence of graphene plane orientation and the finite space from small graphene separation. Both factors affect the organization of the 4-mer isoprene chains, as the peak around zero degree indicated isoprene-graphene parallel alignment. Distance of graphene plane separation was an important factor, as the chance of chain vectors being parallel to the graphene plane was higher with smaller separation distance.

These results indirectly signify the higher possibility of crystalline phase formation when isoprene chains were confined within a smaller gap. Moreover, the drastic change between the highest peak densities at 2.21 and 4.11 separation distances from the local density analysis suggested that there should be a critical separation distance, serving as a transition point between amorphous and crystalline phases of isoprene.

Table 1. graphene concentration, graphene separation distance, total density and rubber density of three simulated systems

Number of 4-mer isoprene	[graphene] (phr)	Graphene Separation (nm)	Total Density ($\text{kg} \cdot \text{m}^{-3}$)	Isoprene Density ($\text{kg} \cdot \text{m}^{-3}$)
a) 30	100	1.24	1228	615
b) 60	50	2.21	1048	699
c) 120	25	4.11	925	740

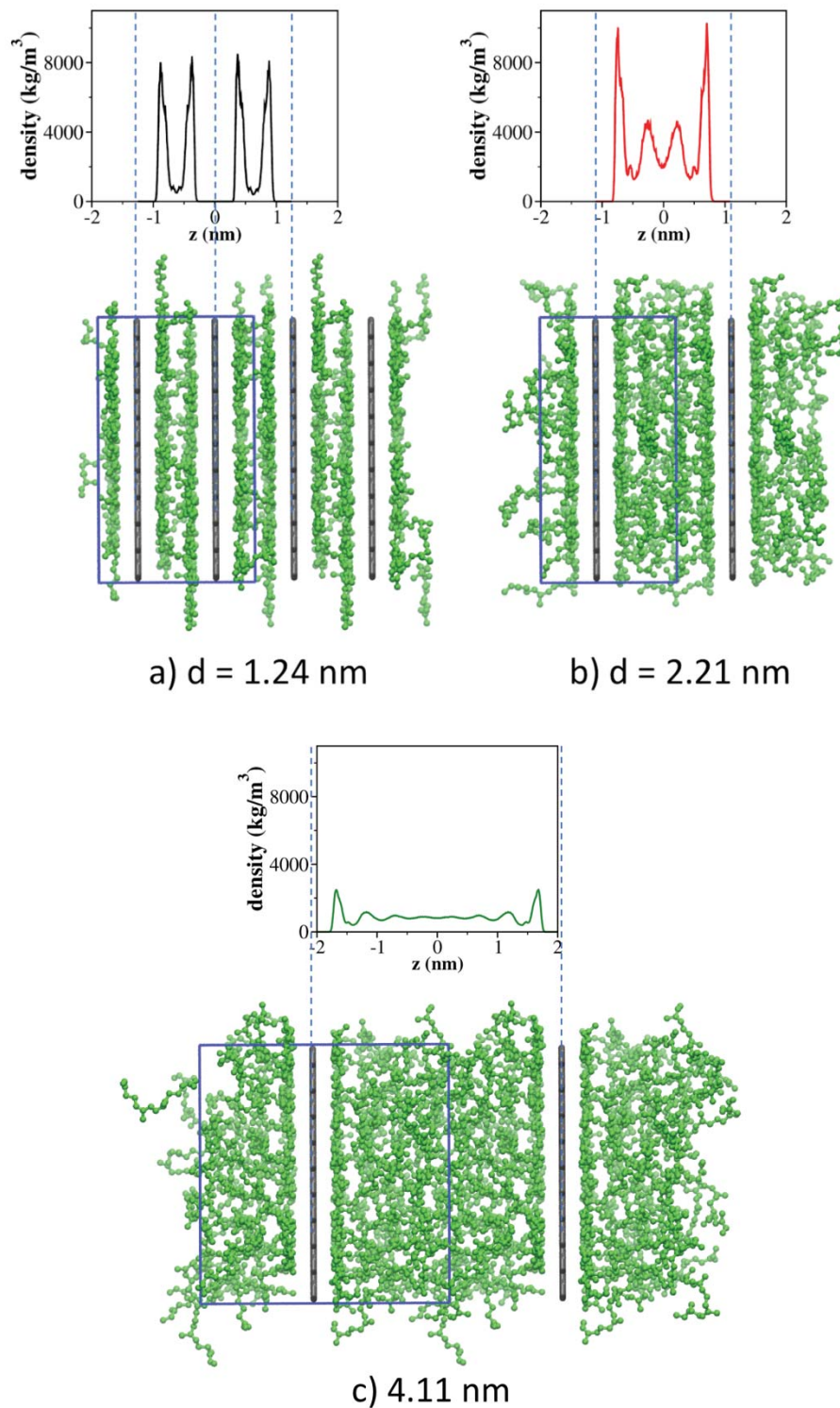


Figure 2. (top) time averaged local density and (bottom) final snapshots from the 50-ns productive MD runs of a) C678 graphene / 30 x (isoprene)₄ with the confinement thickness 1.24 nm, b) C678 graphene / 60 x (isoprene)₄ with the confinement thickness 2.21 nm and c) C678 graphene / 120 x (isoprene)₄ with the confinement thickness 4.11 nm.

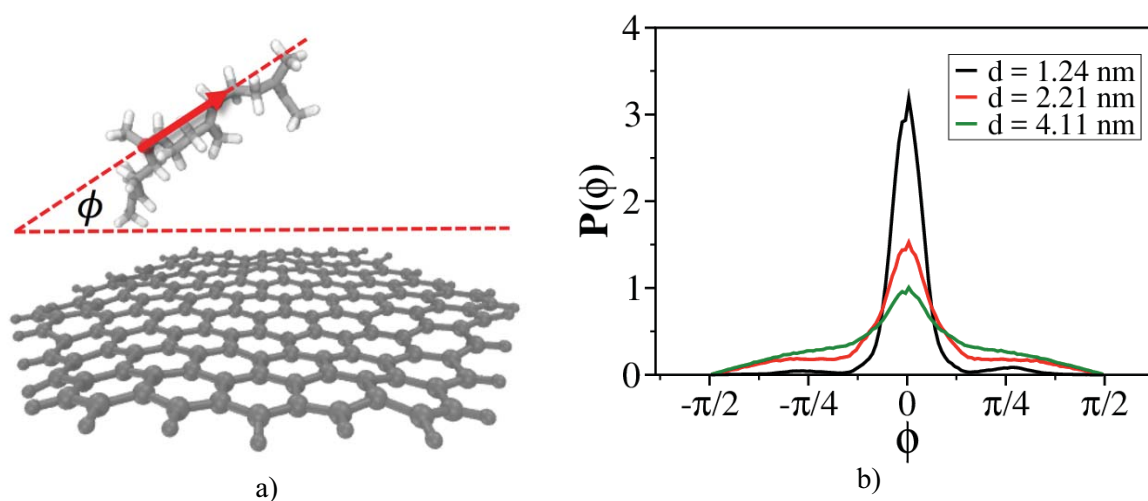


Figure 3: a) a diagram describing the angle made by the graphene plane and a vector pointing from the second monomer to the third monomer of 4-mer isoprene and b) probability distribution of the angle ϕ for each graphene separation distance.

4. Conclusions

A preliminary series of atomistic molecular dynamics simulations of isoprene 4-mer/graphene composite was performed to demonstrate the finite size effect emerged from confining isoprene 4-mer molecules between two graphene sheets. The simulation of 120 isoprene 4-mer/C678 graphene showed that high density shells were formed at the isoprene/graphene interface while the density at further distance from graphene became converged to bulk density. As the size of confinement region was decreased, the density at the interface became significantly higher, but the contribution of rubber mass to global density became lower. These results were accompanied by the measurement of chain orientations. Most of the chains confined within two graphene sheets separated by 1.24 nm were forced to be in parallel with the graphene sheets. The smaller populations of the chains parallel to the graphene plane were measured for the simulations with larger graphene separations, indicating the less ordered phase.

Acknowledgements

W.L. and T.S. were supported by Thailand Center of Excellence in Physics (ThEP).

References

- [1] Azira A A, Kamal M M and Rusop M 2016 Reinforcement of graphene in natural rubber nanocomposite *AIP Conference Proceedings* 1733
- [2] Thaptong P, Sirisinha C, Thepsuwan U and Sae-Oui P 2014 Properties of Natural Rubber Reinforced by Carbon Black-based Hybrid Fillers *Polymer-Plastics Technology and Engineering* **53** 818–23
- [3] Hernández M, Bernal M D M, Verdejo R, Ezquerro T A and López-Manchado M A 2012 Overall performance of natural rubber/graphene nanocomposites *Composites Science and Technology* **73** 40–6
- [4] Yamamoto T 2010 Molecular dynamics simulations of polymer crystallization in highly supercooled melt: Primary nucleation and cold crystallization *The Journal of Chemical Physics* **133** 034904
- [5] Guseva D V, Komarov P V and Lyulin A V 2014 Molecular-dynamics simulations of thin polyisoprene films confined between amorphous silica substrates *The Journal of Chemical Physics* **140** 114903

- [6] Hanwell M D, Curtis D E, Lonie D C, Vandermeersch T, Zurek E and Hutchison G R 2012 Avogadro: an advanced semantic chemical editor, visualization, and analysis platform *Journal of Cheminformatics* **4** 17
- [7] Malde A K, Zuo L, Breeze M, Stroet M, Poger D, Nair P C, Oostenbrink C and Mark A E 2011 An Automated Force Field Topology Builder (ATB) and Repository: Version 1.0 *Journal of Chemical Theory and Computation* **7** 4026–37
- [8] Hess B, Bekker H, Berendsen H J C and Fraaije J G E M 1997 LINCS: A linear constraint solver for molecular simulations *Journal of Computational Chemistry* **18** 1463–72
- [9] Darden T, York D and Pedersen L 1993 Particle mesh Ewald: An N·log(N) method for Ewald sums in large systems *The Journal of Chemical Physics* **98** 10089–92
- [10] Parrinello M and Rahman A 1980 Crystal Structure and Pair Potentials: A Molecular-Dynamics Study *Physical Review Letters* **45** 1196–9
- [11] Abraham M J, Murtola T, Schulz R, Páll S, Smith J C, Hess B and Lindahl E 2015 GROMACS: High performance molecular simulations through multi-level parallelism from laptops to supercomputers *SoftwareX* **1-2** 19–25